

Effects of diffusive property heterogeneity on effective matrix diffusion coefficient for fractured rock

Yingqi Zhang,¹ Hui-hai Liu,¹ Quanlin Zhou,¹ and Stefan Finsterle¹

Received 16 August 2005; revised 15 December 2005; accepted 17 January 2006; published 11 April 2006.

[1] Heterogeneities of diffusion properties are likely to influence the effective matrix diffusion coefficient determined from tracer breakthrough curves. The objectives of this study are (1) to examine if it is appropriate to use a single, effective matrix diffusion coefficient to predict breakthrough curves in a fractured formation, (2) to examine if a postulated scale dependence of the effective matrix diffusion coefficient is caused by heterogeneity in diffusion properties, and (3) to examine whether multirate diffusion results in the previously observed time dependence of the effective matrix diffusion coefficient. The results show that the use of a single effective matrix diffusion coefficient is appropriate only if the interchannel and intrachannel variability of diffusion properties is small. The scale dependence of the effective matrix diffusion coefficient is not caused by the studied types of heterogeneity. Finally, the multirate diffusion process does not result in the time dependence of the effective matrix diffusion coefficient.

Citation: Zhang, Y., H. Liu, Q. Zhou, and S. Finsterle (2006), Effects of diffusive property heterogeneity on effective matrix diffusion coefficient for fractured rock, *Water Resour. Res.*, 42, W04405, doi:10.1029/2005WR004513.

1. Introduction

[2] It is well recognized that matrix diffusion can significantly retard solute transport in fractured rock. Understanding the diffusion of contaminants from fractures into the matrix is essential for predicting the arrival time, maximum contaminant concentration, and the tail of a breakthrough curve (BTC) at a given location. The effective matrix diffusion coefficient, defined as the molecular diffusion coefficient in free water multiplied by matrix tortuosity, is a key parameter in determining matrix diffusion processes. Recent studies have found that effective matrix diffusion coefficients obtained from field-scale tracer tests are significantly larger than those from laboratory measurements [Andersson *et al.*, 2004; Liu *et al.*, 2004a, 2003, 2004b; Neretnieks, 2002; Shapiro, 2001; Zhou *et al.*, 2005]. By compiling effective matrix diffusion values observed from different test sites, Liu *et al.* [2004a] and Zhou *et al.* [2005] reported that the effective matrix diffusion coefficient may be scale dependent and increase with testing scale. However, the mechanisms behind this potential scale dependence are presently not clear.

[3] Water flow and solute transport processes in fractured rock are complicated by heterogeneities at different scales and the complex geometry of fracture networks. Although different conceptual models for flow and transport in fractured rock exist, many studies indicate that the flow pattern is mainly characterized by discrete flow channels [Neretnieks, 2002; Tsang and Neretnieks, 1998]. Fluids in different channels are not very well mixed (at least in a typical field test), except at the influent and

effluent points, where the mixing of different channels is induced by pumping [Neretnieks, 2002]. Different channels having different flow and transport properties induces heterogeneity that impacts contaminant migration. In this study we refer to this kind of heterogeneity as interchannel heterogeneity.

[4] Matrix diffusion processes in fractured rock are conceptually similar to mass transfer processes between “mobile” and “immobile” zones in porous media. The conceptual model of mobile/immobile zones was proposed by Dean [1963] and later extended by van Genuchten and Wierenga [1976]. In this model, the liquid phase in porous media is partitioned into mobile and immobile zones. When the mass transfer is caused purely by molecular diffusion, this mass transfer rate coefficient is conceptually similar to (and thus can be converted to) the effective matrix diffusion coefficient in fractured rock.

[5] There exists an improved version of the mobile/immobile zone model, called the multirate diffusion model [Haggerty and Gorelick, 1995, 1998; van Genuchten *et al.*, 1984]. As a result of heterogeneity at the pore scale, which we refer to as intrachannel heterogeneity, the mass transfer coefficient in the multirate diffusion model is modeled by a distribution of rate coefficients, rather than by a single value. Haggerty and Gorelick [1995] demonstrated that a multirate mass transfer model simultaneously represents various mass transfer processes in a porous medium, and the rate models of mass transfer are mathematically equivalent to the diffusion models of mass transfer. The two most often used distributions of diffusion rate coefficients are the gamma distribution and the lognormal distribution. Haggerty and Gorelick [1998] investigated different distribution functions and concluded that their experimental data were well represented when using a lognormal distribution of diffusion rate coefficients.

[6] Recently, Haggerty *et al.* [2004] compiled a large number of first-order mass transfer rate coefficients

¹Earth Sciences Division, Lawrence Berkeley National Laboratory, University of California, Berkeley, California, USA.

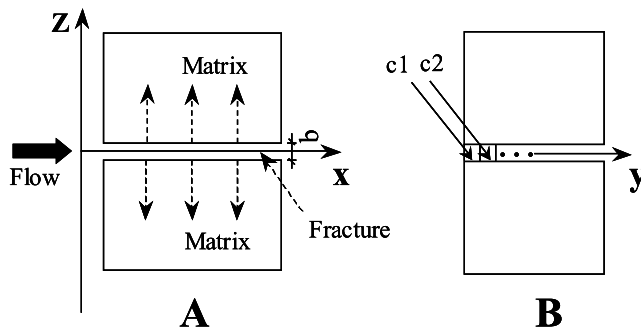


Figure 1. Schematic of a single fracture system [Yamashita and Kimura, 1990].

estimated from test results. They found that the estimated rate coefficient depends on the test duration (t_{exp}) and is correlated to the advection residence time ($t_w = L/v$, where L is the distance from the injection to the effluent point, and v is the average pore water velocity). A larger mass transfer rate coefficient corresponds to a smaller t_{exp} or t_w . One of the possible explanations for the time dependence (given by Haggerty *et al.* [2004]) is that some tests were analyzed using a single-rate diffusion model even though the system exhibited multiple timescales for mass transfer.

[7] Note that multirate diffusion processes have recently been used also for the analysis of tracer transport in fractured rock [Haggerty *et al.*, 2004]. In contrast to the observations of Haggerty *et al.* [2004], Zhou *et al.* [2005] did not find a correlation between test duration and the estimated effective matrix diffusion coefficient for a number of fractured rock sites. Therefore the question arises whether the dependence on test duration for porous media observed by Haggerty *et al.* [2004] also holds for fractured rocks with multiple timescales of mass transfer.

[8] In this paper, we focus on the effects of two types of heterogeneity in diffusion properties (i.e., the interchannel heterogeneity, heterogeneity between individual flow channels, and the intrachannel heterogeneity, heterogeneity within an individual flow channel) on the effective matrix diffusion coefficient for fractured rock. More specifically, our goals are (1) to examine if it is appropriate to use a single effective matrix diffusion coefficient in a standard solution to solute transport to predict BTCs in a fractured formation, and how this effective value is related to the degree of variability of the matrix diffusion coefficient, (2) to examine if the effective matrix diffusion coefficient changes with scale, which would indicate that the observed scale dependence of the effective matrix diffusion coefficient is caused by heterogeneity in diffusion properties, and (3) to examine whether the multirate diffusion process results in the observed time dependence of the effective matrix diffusion coefficient.

[9] The effects of hydrodynamic dispersion are excluded from this study, because the interplay between matrix diffusion and dispersion within the fracture network makes the interpretation of numerical and experimental results difficult and ambiguous. Retardation due to sorption is also ignored in order to be able to separate and identify the effects of matrix diffusion heterogeneity on BTCs in frac-

tured rock. However, in a real system, both dispersion and sorption may be important and should be considered.

2. Problem Setup

[10] A simple fracture system, illustrated in Figure 1, is used in this study. The system consists of a fracture oriented in the x direction, embedded in matrix rock. Figure 1a shows a cross-sectional view of the fracture in the x - z plane, and Figure 1b shows the y - z plane. Flow is one-dimensional in the x direction. The fracture aperture is denoted as b , and a unit length is taken in the y direction. Water is assumed to flow along the fracture with a constant velocity. Tracer is applied using a Dirac input function, i.e., a contaminant of mass M_0 is instantaneously released at location $x = 0$ and time $t = 0$, so the concentration at $x = 0$ is:

$$c_0 = \frac{M_0}{bv} \delta(t) \quad (1)$$

where v is the flow velocity and $\delta(t)$ is the Dirac delta function. While most of the contaminant is advectively transported in the fracture, some contaminant mass is transferred from the fracture into the matrix by molecular diffusion. In our numerical experiments, we assume a negligible hydrodynamic dispersion (local dispersion) in the fracture and use a conservative tracer. We also assume complete mixing across the fracture aperture. Matrix porosity is 0.15, fracture aperture is 4.0×10^{-5} m, flow velocity is 2.5×10^{-3} m/s, and a unit contaminant mass of 1g and a unit width of fracture of 1m are taken for our calculation. For a single-fracture system, we assume the matrix block size is larger than the diffusion penetration depth (which is on the order of $2\sqrt{D_m t_{\text{exp}}}$, where D_m is the matrix diffusion coefficient). This estimate needs to be adjusted for different fracture network geometries (e.g., the applicable matrix block size is twice as large in a parallel-fracture system). The assumption of an essentially infinite diffusion capacity on the timescale of interest enables us to ignore the impact of a finite matrix block size.

[11] On the basis of these assumptions, the solution to the transport equation subject to the above Dirac input injection is given by Tang *et al.* [1981]:

$$c(x, t) = \frac{M_0 k}{bv\sqrt{\pi}(t - t_w)^{3/2}} \exp\left(-\frac{k^2}{t - t_w}\right), \quad t > t_w \quad (2)$$

where: $c(x, t)$ is the contaminant concentration at location x and time t ; $t_w = L/v$ is the residence time, where L is the distance between the contaminant release point and location x ; and $k = \frac{\phi_m \sqrt{D_m t_w}}{b}$, where ϕ_m is the matrix porosity.

3. Interchannel Heterogeneity

[12] Flow and transport processes in fractured rock occur along individual flow channels within a fracture network [Neretnieks, 2002]. As mentioned above, interchannel heterogeneity results from different flow channels having different flow and transport properties. In this study, we use a simplified conceptual flow model to investigate the effects of interchannel heterogeneity on diffusive properties. Specifically, we consider a simplified multichannel system,

in which each flow channel has uniform properties and does not mix with any other channels except at influent and effluent points. These channels have the same length, width, fracture aperture, and other properties, but different matrix diffusion coefficients.

[13] *Haggerty et al.* [2001] suggested that the distribution of diffusion rate coefficients may be defined in any appropriate manner. Most commonly, diffusion rate coefficients are characterized by a statistical distribution. For interchannel heterogeneity, we investigate two kinds of distributions for matrix diffusion coefficient. First, we assume a distribution that allows us to derive an analytical solution at the effluent point, given the solution for a single-channel flow system. Then we compare the form of the analytical solution with the single-channel model to see whether specifying a single effective matrix diffusion coefficient is appropriate to capture transport and matrix diffusion when interchannel heterogeneity exists. Even though the assumption of this distribution may not be physically justified, we nevertheless can obtain some insights from the corresponding analytical solution. Secondly, we use a lognormal distribution, as suggested by *Haggerty et al.* [2001]. A numerical experiment is performed to examine the existence and appropriateness of using a single effective matrix diffusion coefficient.

[14] For the first analysis, we define $a = \frac{k}{t_w} = \frac{\phi_m \sqrt{D_m}}{b}$ (see equation (2)), and assume a follows a normal distribution (which is equivalent to $\sqrt{D_m}$ having a normal distribution, since ϕ_m and b are considered constant). When $t > t_w$ we can rewrite equation (2) as

$$c(x, t) = \frac{M_0 t_w a}{bv\sqrt{\pi}(t - t_w)^{3/2}} \exp\left(-\frac{t_w^2 a^2}{t - t_w}\right) \quad (3)$$

[15] The probability density function for a is given by

$$f(a) = \frac{1}{\sigma\sqrt{2\pi}} \exp\left[-\frac{(a - \bar{a})^2}{2\sigma^2}\right] \quad (4)$$

where σ is the standard deviation of a , and \bar{a} is the arithmetic mean of a . So the average concentration at the effluent point is

$$\begin{aligned} \bar{c}(x, t) &= \frac{M_0 t_w}{bv\sqrt{\pi}(t - t_w)^{3/2}} \int_{-\infty}^{+\infty} \frac{a}{\sigma\sqrt{2\pi}} \exp\left[-\frac{t_w^2 a^2}{t - t_w} - \frac{(a - \bar{a})^2}{2\sigma^2}\right] da \\ &= \frac{M_0 t_w \bar{a}}{bv\sqrt{\pi}(t - t_w + 2t_w^2 \sigma^2)^{3/2}} \exp\left[-\frac{t_w^2 \bar{a}^2}{t - t_w + 2t_w^2 \sigma^2}\right] \end{aligned} \quad (5)$$

Let $T_w = t_w - 2t_w^2 \sigma^2$. Inserting T_w into equation (5) yields

$$\bar{c}(x, t) = \frac{M_0}{bv\sqrt{\pi}(t - T_w)^{3/2}} \exp\left[-\frac{\left(\frac{T_w}{1 - 2t_w \sigma^2}\right)^2 \bar{a}^2}{t - T_w}\right] \quad (6)$$

Comparing equations (3) and (6), we can conclude that unless (1) the standard deviation is very small, and (2) t_w is very small (which means advection dominates and the effects of diffusion can be ignored), a single effective matrix

diffusion coefficient is unlikely to exist for the analytical solution given by equation (3).

[16] This analysis assumed that the square root of the matrix diffusion coefficient is normally distributed. This assumption implies that negative values of $\sqrt{D_m}$ are allowed, which is physically not possible. Consequently, it may be more reasonable to assume a lognormal distribution for the matrix diffusion coefficient (for details, see *Haggerty et al.* [2001]). In the second analysis, we use a Monte Carlo method, in which the matrix diffusion coefficient for each channel is sampled from a lognormal distribution. Then the BTC for each channel is calculated and an average BTC is obtained. This is an alternative method to numerically integrating equation (3) over the distribution of matrix diffusion coefficient. Sampling the distribution by the Latin hypercube method is conceptually similar to discretizing the distribution during numerical integration of equation (3). An effective matrix diffusion coefficient is determined by fitting the BTC calculated using equation (2) to this average BTC, assuming complete mixing at the effluent point. This step is conducted using iTOUGH2-TRAT [Zhou, 2005]. The iTOUGH2-TRAT program was developed to calibrate transport parameters using BTCs observed in field (or laboratory) tracer tests. It is based on iTOUGH2, a program using inverse modeling for parameter estimation and uncertainty analysis [Finsterle, 1999]. Six analytical models for tracer transport with different flow configurations and boundary conditions are implemented in iTOUGH2-TRAT. For our calibration purpose, we use the analytical solution for a single fracture embedded in a porous rock without dispersion as given by *Tang et al.* [1981] (see also equation (2)).

[17] In the numerical experiment we use a mean of -12 for $\ln(D_m)$, where D_m has units of m^2/h , corresponding to a geometric mean of D_m of $1.71 \times 10^{-9} \text{ m}^2/\text{s}$. For the base case, we assume a standard deviation for $\ln(D_m)$ of 0.598, which yields an arithmetic mean for D_m of $2.04 \times 10^{-9} \text{ m}^2/\text{s}$ (these values and the matrix porosity are taken from *Fleming and Haggerty* [2001]). These relatively large values come from the vuggy porosity). Three effluent points at $L = 5 \text{ m}$, 50 m , and 500 m are used in the numerical experiment.

[18] The calibrated effective matrix diffusion coefficient is $1.58 \times 10^{-9} \text{ m}^2/\text{s}$ for all three effluent points. The sampling of the matrix diffusion coefficient for a given distribution is performed using Latin Hypercube sampling (LHS) [McKay et al., 1979; Iman and Conover, 1982], a method that is more efficient than the traditional Monte Carlo method. In this method, the probability distribution curve for a variable is divided into N_{LHS} intervals of equal probability, where N_{LHS} is equal to the total number of realizations being generated. Then, a realization is sampled from each interval.

[19] A total of 10 channels are used in the analysis. Increasing the number of channels does not change the estimated matrix diffusion coefficient significantly (e.g., for the base case, the calibrated value changes only slightly to $1.575 \times 10^{-9} \text{ m}^2/\text{s}$ for 50,000 channels); 10 channels are therefore considered reasonable.

[20] In Figure 2a we plot both the average BTC from all channels and the BTC from equation (2) using the calibrated effective matrix diffusion coefficient for the effluent point at $L = 5$. For a standard deviation of 0.598, the calibrated

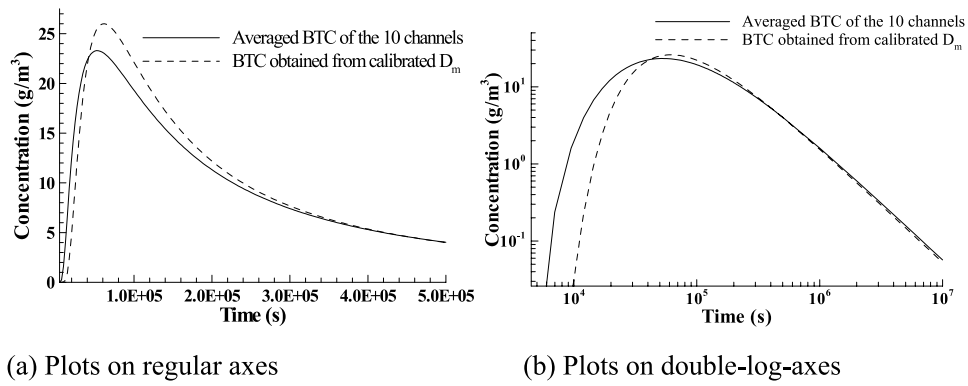


Figure 2. Average BTC of the 10 channels versus the BTC from the regular-space-calibrated D_m for the base case. (a) Plots on regular axes. (b) Plots on double-log axes.

curve does not fit the peak well, whereas the tail is very well reproduced. The root mean square error (defined as $RMSE = \left[\sum_m r^2 / (m - n) \right]^{1/2}$, where r is the residual at each calibration point, $m = 200$ is the total number of calibration points, and $n = 1$ is the number of estimated parameters) is 1.81, which is approximately 8% of the peak and 20% of the average concentration values (integration of concentration over time divided by time on the BTC). Whether such an average fitting error ($RMSE = 1.81$) is acceptable depends on the prediction accuracy required by the specific application.

[21] The question arises whether the log concentrations should be analyzed and whether sampling should occur equally or logarithmically spaced in time. These choices affect the relative weighting of early breakthrough, peak values, or small concentrations in the tail of the BTC. We chose to perform the analysis in regular rather than logarithmic space. Taking the logarithm of concentration not only down weighs the peak concentration, but may also put undue weight on very small concentrations at early and very late times, causing difficulties during the inversion and potentially biasing the estimates. To illustrate this effect, we show the same case with the analysis done on double-log axes. The results are plotted both on regular axes (Figure 3a) and double-log axes (Figure 3b). For the comparison we also plot the fitting curves using regular-space-calibrated D_m on double-log axes as shown in Figure 2b. Comparison of Figures 2 and 3 indicates that fitting D_m in regular space yields better predictions of both the peak concentration and

the tail. The calibration of log-log data obviously leads to a bias in the estimated parameters. We therefore consider the regular axes analysis to be more appropriate. Figures 2b and 3b also illustrate the sensitivity of the BTCs to changes in the matrix diffusion coefficient ($D_m = 1.58 \times 10^{-9}$ m²/s and 8.87×10^{-10} m²/s, respectively).

[22] The analysis was repeated for standard deviations of 0.3 and 0.8. A good fit is achieved and acceptable for a standard deviation of 0.3, but not for 0.8. When the standard deviation is 0.3, the differences between the calibrated effective matrix diffusion coefficients evaluated at the three effluent points are insignificant, i.e., no scale dependence is observed. Therefore, for a standard deviation on the order of 0.3, an effective matrix diffusion coefficient can be found and used to estimate the entire BTC. Moreover, when $\ln(D_m)$ has a standard deviation on the order of 0.6, an effective matrix diffusion coefficient may be found and used to estimate the tail of the BTC. However, if the peak of the BTC is very important, this single effective value cannot be used. When the standard deviation of $\ln(D_m)$ is small and the single effective matrix diffusion coefficient can be estimated, no scale dependence of matrix diffusion coefficients caused by small interchannel heterogeneity can be observed.

4. Intrachannel Heterogeneity

[23] In addition to interchannel heterogeneity, variability in diffusive mass transfer properties within a flow channel also plays an important role for solute transport. In this

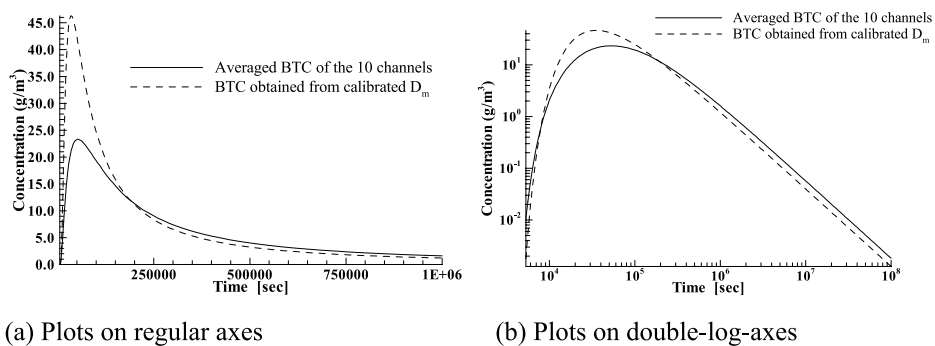


Figure 3. Average BTC of the 10 channels versus the BTC from the log-space-calibrated D_m for the base case. (a) Plots on regular axes. (b) Plots on double-log axes.

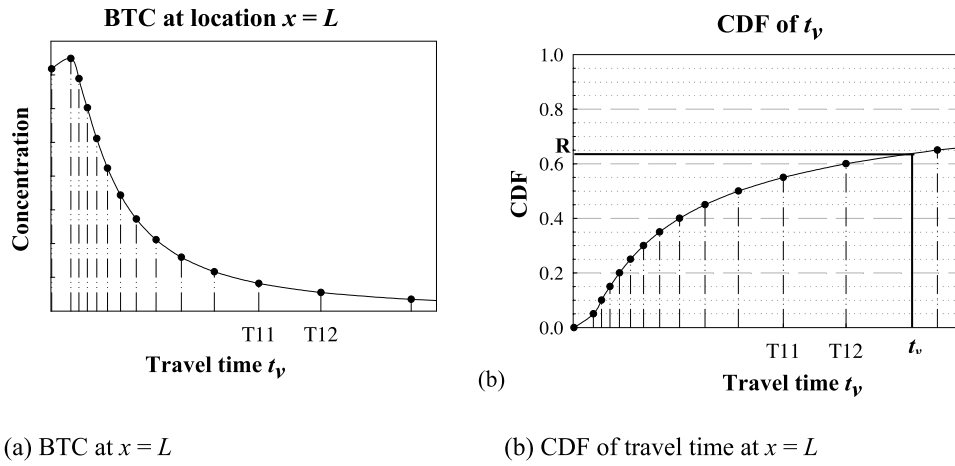


Figure 4. Illustration of the particle-tracking method. (a) BTC at $x = L$. (b) CDF of traveltime at $x = L$.

study, we apply a particle-tracking method to capture the intrachannel heterogeneity of the matrix diffusion coefficient. The particle-tracking method has been used in many studies for different purposes [Tsang and Doughty, 2003; Tsang and Tsang, 2001; Yamashita and Kimura, 1990]. On the basis of the approach of Yamashita and Kimura [1990] we incorporate the intrachannel heterogeneity of the matrix diffusion coefficient into a particle-tracking framework to solve tracer transport through a single fracture.

[24] Given the solution in equation (2), we can integrate the mass flux $F = cbv$ from $t = 0$ to t_v , which yields

$$\int_0^{t_v} F(L, t) dt = M_0 \operatorname{erfc}\left(\frac{k}{\sqrt{t_v - t_w}}\right) \quad (7)$$

As t_v goes to infinity, this integration converges to the total released mass M_0 . The ratio F/M_0 can be treated as the probability density function of the contaminant traveltime, and $\operatorname{erfc}\left(\frac{k}{\sqrt{t_v - t_w}}\right)$ is the cumulative distribution function (CDF) for the contaminant traveltime. This is the starting point of the particle-tracking method suggested by Yamashita and Kimura [1990] to solve radionuclide transport in fractured porous media. The basic idea of the method is illustrated in Figure 4, where Figure 4a represents a BTC at location $x = L$ and Figure 4b represents the corresponding CDF for the contaminant traveltime. In both Figures 4a and 4b, contaminant traveltime is plotted on the x axis. Assume that we divide the CDF of the traveltime into 20 equal intervals as shown in Figure 4b (only part of the CDF is shown because the curve gets very flat as it approaches 1) and find the corresponding traveltime interval Δt_v (time length between two adjacent times of the CDF).

[25] The procedure of the particle-tracking method includes the following steps.

[26] 1. Release a total number of N particles at $x = 0$.

[27] 2. For each particle, generate a random number R from a uniform distribution in the interval $[0, 1]$, and solve for the particle traveltime t_v from (see Figure 4b):

$$R = \operatorname{erfc}\left(\frac{k}{\sqrt{t_v - t_w}}\right) \quad (8)$$

Repeat step 2 for all N particles.

[28] 3. Determine the experiment end time t_{end} (the traveltime of the slowest particle to reach the effluent point). Plot the histogram of particle arrival times.

[29] 4. Given that M particles arrive at $x = L$ between times t_1 and t_2 , the average concentration at $x = L$ at time $t = (t_1 + t_2)/2$ is calculated as

$$c_0 = \frac{M}{N} \frac{M_0}{bv(t_2 - t_1)} \quad (9)$$

The average concentration is calculated for each time interval, resulting in the BTC at $x = L$.

[30] The procedure as outlined was developed for systems with constant D_m . We slightly modified the procedure to consider intrachannel heterogeneity, where D_m is different at different locations. We divide the flow path along the fracture into small segments. The flow path encountered by a particle consists of segments with varying matrix diffusion coefficients, and each particle follows a separate flow path. A local D_m (sampled from a distribution curve) is assigned to each segment along the particle's path. Then the traveltime in this segment is calculated for each particle, and the procedure is repeated for each segment. Finally, at the observation point $x = L$, the traveltimes in all segments are added for each particle, which is the traveltime for the particle to travel from $x = 0$ to $x = L$, and the BTC can be calculated for $x = L$. This modified particle tracking method was chosen because it is conceptually easy to understand.

[31] A lognormal distribution is used to characterize the intrachannel heterogeneity of the matrix diffusion coefficient. The statistics (e.g., the mean and the variance of $\ln(D_m)$) describing the base case intrachannel heterogeneity are assumed to be the same as those used for describing the base case interchannel heterogeneity. Note that in general the variance of the intrachannel heterogeneity is expected to be smaller than that of the interchannel heterogeneity, which refers to a somewhat larger scale. The impact of the variance on the estimated effective matrix diffusion coefficients is examined through sensitivity analyses. A total of 50,000 particles is used in our modified particle-tracking method. This number is considered sufficient to yield stable output statistics, as is confirmed by Yamashita and Kimura [1990], who did not observe significant differences when using either 20,000 or 200,000 particles.

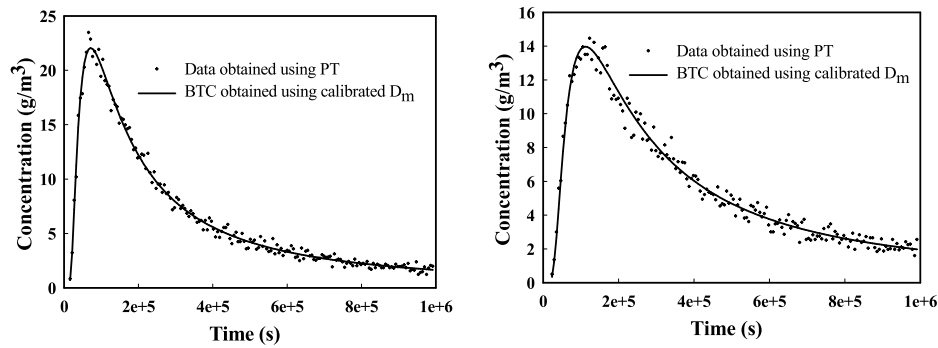


Figure 5. Simulated BTC using particle tracking versus the BTC from the calibrated effective matrix diffusion coefficient: (left) $s = 0.598$ and (right) $s = 1.5$.

[32] The length of a segment used in the calculation is 0.05 m. To test the sensitivity of the results to the discretization of the flow path, a high-resolution simulation was performed, in which the flow path of length $L = 5$ m was subdivided into one million segments. The difference between the resulting estimates of the effective matrix diffusion coefficient (2.99×10^{-9} m²/s versus 3.04×10^{-9} m²/s) is considered insignificant.

[33] Figure 5 shows fitting plots at $L = 5$ m, i.e., the simulated BTC of the heterogeneous system obtained using the particle-tracking method, and the BTC for an equivalent homogeneous system obtained using equation (2) and the calibrated, effective matrix diffusion coefficient. Figure 5 gives the results for standard deviations of 0.598 (Figure 5, left) and 1.5 (Figure 5, right) (corresponding to an arithmetic mean for D_m of 2.04×10^{-9} m²/s and 5.26×10^{-9} m²/s), leading to RMSEs of 0.485 and 0.497, respectively. The generally good fit indicates that the heterogeneous system behavior can be reasonably well represented by a homogeneous system with an appropriate effective diffusion parameter. The analysis was repeated by increasing the standard deviations of $\ln(D_m)$ stepwise up to 4.0. Good matches were obtained for standard deviations up to 2.0. For higher standard deviations, equation (2) is no longer capable of capturing the shape of the entire BTC from the heterogeneous system, leading to a minor mismatch (underprediction) at early times, which is compensated for in a least squares sense by an overprediction of the peak concentration value. Again, whether this mismatch is acceptable depends on the application, e.g., whether arrival time or peak values are of interest. The estimated effective matrix diffusion coefficient can be used to estimate the tail of the BTC. When the standard deviation is above 4.0, an obvious mismatch is observed, and the estimated effective parameter should not be used.

[34] The calibrated effective matrix diffusion coefficients for standard deviations of 0.598 and 1.5 are listed in Table 1. Similar to the interchannel heterogeneous cases with small variances, the differences among the calibrated matrix diffusion coefficients at different effluent points are not sufficient to indicate scale dependence of the matrix diffusion coefficient. This observation is independent of the variance. Thus the intrachannel heterogeneity is not the reason for the observed scale dependence of the effective matrix diffusion coefficient.

[35] On the basis of our numerical experiments, when the standard deviation of $\ln(D_m)$ is less than 4.0, the following empirically determined formula can be used to estimate the effective matrix diffusion coefficient in the presence of lognormally distributed intrachannel heterogeneity:

$$\hat{D}_m = \exp \left[m + \frac{s^2}{4} \right] \quad (10)$$

where m and s are the mean and the standard deviation of $\ln(D_m)$, respectively. Figure 6 shows that equation (10) can be used to estimate the effective matrix diffusion coefficient up to a standard deviation of $s = 2$ for all applications, and up to $s = 3$ for applications where the minor mismatch at the peak can be ignored. Recall that for higher standard deviations, the use of an effective matrix diffusion coefficient is questionable, because equation (2) is an unlikely model of the heterogeneous system.

[36] The coefficient \hat{D}_m calculated using equation (10) is very close to the effective matrix diffusion coefficient (\bar{D}_m) when s is less than 2 (e.g., when $s = 2$, $\hat{D}_m = 4.62 \times 10^{-9}$ m²/s versus $\bar{D}_m = 4.64 \times 10^{-9}$ m²/s). Again, as we continue to increase s , the difference between the calculated and the calibrated values starts to increase. Figure 7 is an illustration of three BTCs (at $L = 5$ m and for $s = 3$): the black dots are the simulated data using the modified particle-tracking method, the blue line is the BTC obtained by inserting the calibrated effective matrix diffusion coefficient into equation (2), and the red line is the BTC obtained using \hat{D}_m estimated by equation (10). Neither the calibrated diffusion coefficient nor that estimated by equation (10) give a perfect match to the peak concentration from the heterogeneous system; however, they both match the tail very well.

[37] As previously mentioned, *Haggerty et al.* [2004] reported that the mass transfer coefficient in porous media

Table 1. Effective Matrix Diffusion Coefficient With Intrachannel Heterogeneity^a

| Standard Deviation of $\ln(D_m)$ | $L = 5$ m | $L = 50$ m | $L = 500$ m |
|----------------------------------|-----------------------|-----------------------|-----------------------|
| 0.598 | 1.86×10^{-9} | 1.83×10^{-9} | 1.87×10^{-9} |
| 1.5 | 2.99×10^{-9} | 2.96×10^{-9} | 2.99×10^{-9} |

^aValues are in m²/s.

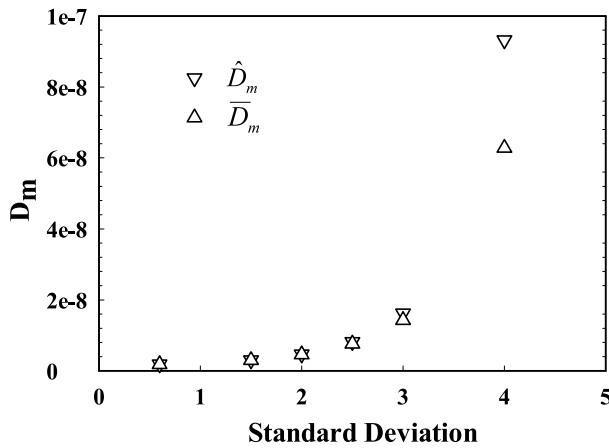


Figure 6. \hat{D}_m calculated using equation (10) versus calibrated \bar{D}_m using equation (2) for different standard deviation s .

decreases with test duration, but the trend is not obvious for fractured media (see their Figure 1). Recall that their mass transfer coefficient is conceptually similar to the effective matrix diffusion coefficient used here. Zhou *et al.* [2005] indicated that the test duration dependency is not evident from the analysis of tracer tests conducted in fractured rocks. In these intrachannel heterogeneity experiments with the modified particle-tracking method, we also investigate the relationship between test duration and effective matrix diffusion coefficient for multirate diffusion processes by varying the advection residence time t_w for a flow channel with a lognormal distribution of the matrix diffusion coefficient at each location. In addition to the base case (with $L = 50$ m and $s = 0.598$, which results in a residence time of $t_w = 2.0 \times 10^4$ s), we run four cases with advection residence times t_w of 2.0×10^3 s, 2.0×10^5 s, 2.0×10^6 s, and 2.0×10^7 s, respectively. Tests using the same range of advective velocities are done for $L = 5$ m and $L = 500$ m. The resulting effective matrix diffusion coefficients are identical for different advection residence times (or test durations). The results indicate that the multirate diffusion process from pore-scale heterogeneity cannot explain the dependence of the effective matrix diffusion coefficient on test duration, at least not for fractured rock. This result is consistent with the finding of Zhou *et al.* [2005]. A possible reason for the dependence on test duration observed by Haggerty *et al.* [2004] is that the mass transfer coefficient is overestimated using first-order approximation during early periods of the experiment, since at an early stage, the concentration gradient at the interface between the mobile and immobile zone is much sharper than at later stages of the experiment.

5. Discussion and Conclusion

[38] In this paper, we have investigated how two types of heterogeneity in diffusion properties affect solute transport, namely, interchannel heterogeneity and intrachannel heterogeneity. Our first objective was to examine whether it is appropriate to use a single effective matrix diffusion coefficient, in combination with a standard solution model for transport in a homogeneous medium, to predict BTCs in a

heterogeneous fractured formation. It appears that for both types of heterogeneity we studied, the use of a homogeneous model with an effective matrix diffusion coefficient is appropriate only if the variability is small, e.g., standard deviation of $\ln(D_m)$ for interchannel heterogeneity smaller than 0.3–0.6, and standard deviation of $\ln(D_m)$ for intrachannel heterogeneity smaller than 2.0–4.0, assuming a lognormal distribution of the underlying matrix diffusion coefficient. The lower bound should be used for applications where the prediction of both peaks and tails is important, and the upper bound could be used when the tail is of primary interest. The application range of the effective matrix diffusion coefficient for the interchannel heterogeneity seems to be much smaller than that for intrachannel heterogeneity. Fortunately, a property usually has larger variability when it is averaged over a smaller geological area. For intrachannel heterogeneity, when the use of an effective matrix diffusion coefficient is appropriate, it can be estimated from equation (10), provided that the standard deviation of the underlying matrix diffusion coefficient distribution is known.

[39] The second objective of the study was to examine if the observed scale dependence of the effective matrix diffusion coefficient is caused by heterogeneity in diffusive properties. For both types of heterogeneity, we compared the single effective matrix diffusion coefficients at different effluent points assuming a relatively small variance of $\ln(D_m)$. The difference among the resulting values is small and cannot be considered a consequence of the different study scales. We conclude that the scale dependence is not caused by interchannel or intrachannel heterogeneity in the diffusion coefficient. However, it is possible that in some tracer tests or field experiments, particles may not encounter the entire spectrum of diffusion-relevant matrix properties. In other words, the sampling of the local matrix diffusion coefficient may not be complete, which results in a bias in the actual distribution of the matrix diffusion coefficient. The bias may result in an observed scale dependence.

[40] The third objective of the study was to examine whether the multirate diffusion process actually results in the observed time dependence of the effective matrix diffusion coefficient. We compared the effective matrix

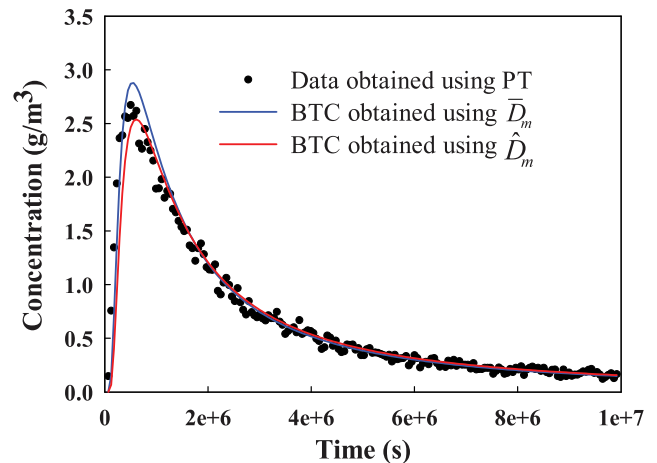


Figure 7. Comparison of simulated concentration using particle tracking (PT, black dots), BTC obtained using \bar{D}_m (blue line), and BTC obtained using \hat{D}_m (red line).

diffusion coefficients for different advection residence times. Again, no significant difference was observed. The results show that multidiffusion processes cannot cause the test duration dependence of the effective matrix diffusion coefficient.

[41] The BTC is affected by both advection through the fracture and retardation caused by diffusion into the matrix. The relative importance of advective and diffusive processes depends on the timescale of interest, i.e., advection dominates at early times, and diffusion dominates at late times. Also note that while the base case advective velocity used in the analysis is relatively large, the matrix diffusion coefficient and the matrix porosity are also relatively large. Moreover, the analysis was performed for a wide range of flow velocities, leading to residence times between 2.0×10^3 s and 2.0×10^7 s, thus examining both advection- and diffusion-dominated systems.

[42] The multichannel model was used to incorporate the interchannel heterogeneity, and the particle-tracking method was used to incorporate the intrachannel heterogeneity. The impacts of these two types of heterogeneity have been studied separately, even though they are unlikely to be distinguished in the results of laboratory and field tracer tests. The study still helps us to understand the role of heterogeneity in matrix diffusion processes.

[43] **Acknowledgments.** Comments by Christine Doughty at Lawrence Berkeley National Laboratory (LBNL) and three anonymous reviewers are greatly appreciated. This work is supported by Office of Science and Technology and International, Office of Civilian Radioactive Waste Management, U.S. Department of Energy contract DE-AC02-05CH11231.

References

- Andersson, P., J. Byegard, E. L. Tullborg, T. Doe, J. Hermanson, and A. Winberge (2004), In situ tracer tests to determine retention properties of a block scale fracture network in granitic rock at the Aspo Hard Rock Laboratory, Sweden, *J. Contam. Hydrol.*, *70*(3–4), 271–297.
- Dean, H. H. (1963), A mathematical model for dispersion in the direction of flow in porous media, *Soc. Pet. Eng. J.*, *3*, 49–52.
- Finsterle, S. (1999), iTOUGH2 user's guide, *Rep. LBNL-40040*, Lawrence Berkeley Natl. Lab., Berkeley, Calif.
- Fleming, S., and R. Haggerty (2001), Modeling solute diffusion in the presence of pore-scale heterogeneity: Method development and an application to the Culebra dolomite member of the Rustler Formation, New Mexico, USA, *J. Contam. Hydrol.*, *48*, 253–276.
- Haggerty, R., and S. M. Gorelick (1995), Multiple-rate mass transfer for modeling diffusion and surface reactions in media with pore-scale heterogeneity, *Water Resour. Res.*, *31*(10), 2383–2400.
- Haggerty, R., and S. M. Gorelick (1998), Modeling mass transfer processes in soil columns with pore-scale heterogeneity, *Soil Sci. Soc. Am. J.*, *62*(1), 62–74.
- Haggerty, R., S. W. Fleming, L. C. Meigs, and S. A. McKenna (2001), Tracer tests in a fractured dolomite: 2. Analysis of mass transfer in single-well injection-withdrawal tests, *Water Resour. Res.*, *37*(5), 1129–1142.
- Haggerty, R., C. F. Harvey, C. Freiherr von Schwerin, and L. C. Meigs (2004), What controls the apparent timescale of solute mass transfer in aquifers and soils? A comparison of experimental results, *Water Resour. Res.*, *40*, W01510, doi:10.1029/2002WR001716.
- Iman, R. L., and W. J. Conover (1982), A distribution-free approach to inducing rank correlation among input variables, *Commun. Stat.*, *11*, 311–334.
- Liu, H. H., C. B. Haukwa, C. F. Ahlers, G. S. Bodvarsson, A. L. Flint, and W. B. Guertel (2003), Modeling flow and transport in unsaturated fractured rock: An evaluation of the continuum approach, *J. Contam. Hydrol.*, *62*(3), 173–188.
- Liu, H. H., G. S. Bodvarsson, and G. Zhang (2004a), Scale dependency of the effective matrix diffusion coefficient, *Vadose Zone J.*, *3*(1), 312–315.
- Liu, H. H., R. Salve, J. S. Wang, G. S. Bodvarsson, and D. Hudson (2004b), Field investigation into unsaturated flow and transport in a fault: model analyses, *J. Contam. Hydrol.*, *74*(1–4), 39–59.
- McKay, M. D., W. J. Conover, and R. J. Beckman (1979), A comparison of three methods for selecting values of input variables in the analysis of output from a computer code, *Technometrics*, *21*, 239–245.
- Neretnieks, I. (2002), A stochastic multi-channel model for solute transport—Analysis of tracer tests in fractured rock, *J. Contam. Hydrol.*, *55*(3–4), 175–211.
- Shapiro, A. M. (2001), Effective matrix diffusion in kilometer-scale transport in fractured crystalline rock, *Water Resour. Res.*, *37*(3), 507–522.
- Tang, D. H., E. O. Frind, and E. A. Sudicky (1981), Contaminant transport in fractured porous media: Analytical solution for a single fracture, *Water Resour. Res.*, *17*(3), 555–564.
- Tsang, C. F., and C. Doughty (2003), A particle-tracking approach to simulating transport in a complex fracture, *Water Resour. Res.*, *39*(7), 1175, doi:10.1029/2001WR001249.
- Tsang, C. F., and I. Neretnieks (1998), Flow channeling in heterogeneous fractured rocks, *Rev. Geophys.*, *36*(2), 275–298.
- Tsang, Y. W., and C. F. Tsang (2001), A particle-tracking method for advective transport in fractures with diffusion into finite matrix blocks, *Water Resour. Res.*, *37*(3), 831–835.
- van Genuchten, M. T., and P. J. Wierenga (1976), Mass transfer studies in sorbing porous media I. Analytical solutions, *Soil Sci. Soc. Am. J.*, *40*(4), 473–480.
- van Genuchten, M. T., D. H. Tang, and R. Guennelon (1984), Some exact solutions for solute transport through soils containing large cylindrical macropores, *Water Resour. Res.*, *20*(3), 335–346.
- Yamashita, R., and H. Kimura (1990), Particle-tracking technique for nuclide decay chain transport in fractured porous media, *J. Nucl. Sci. Technol.*, *27*(11), 1041–1049.
- Zhou, Q. (2005), Software management report for iTOUGH2-TRAT, version 1.0, *Rep. 1001-SMR-1.0-00*, Lawrence Berkeley Natl. Lab., Berkeley, Calif.
- Zhou, Q., H. Liu, F. Molz, Y. Zhang, and G. S. Bodvarsson (2005), Field-scale effective matrix diffusion coefficient for fractured rock: Results from literature survey, *Rep. LBNL-57368*, Lawrence Berkeley Natl. Lab., Berkeley, Calif.

S. Finsterle, H. Liu, Y. Zhang, and Q. Zhou, Earth Sciences Division, Lawrence Berkeley National Laboratory, University of California, MS 90R1116, 1 Cyclotron Road, Berkeley, CA 94720-8126, USA. (yqzhang@lbl.gov)